

## EFFECTS OF THREE-DIMENSIONALITY FOR AN OSCILLATING-WING POWER-GENERATOR

Ferhat Karakas<sup>1</sup> and Idil Fenercioglu<sup>2</sup>  
Istanbul Technical University  
Istanbul, Turkey

### ABSTRACT

*Flow structures around and in the near wake of an oscillating-wing power-generator undergoing non-sinusoidal pitch and plunge motions were investigated for various motion parameters. Flow visualizations are performed to reveal the spanwise flow structure evolution of a non-profiled flat plate. The study is performed in a water channel at chord length based  $Re = 10\,000$  using the DPIV (Digital Particle Image Velocimetry) technique in line with direct force measurements. Quantitative flow visualizations are performed for three different planes along the span of the test model to comment on the three dimensionality effects. The flat plate oscillates with non-sinusoidal pitch leading plunge motions with phase angle of  $\phi = 90^\circ$  about its  $0.44c$  pitch pivot point from the leading edge with stroke reversal times of  $0.1$  (rapid reversal) to  $0.5$  (sinusoidal reversal). The kinematic motion is conducted at fixed reduced frequency of  $k = 0.8$  with plunge amplitude of  $1.05$  chord and pitch amplitude of  $73^\circ$ .*

### INTRODUCTION

Power can be extracted from the flowing fluids in different ways. Using flapping wings is an alternative to conventional power generators. Renewable and sustainable clean energy harvesters are gaining more and more attention and new designs are under development over several decades. The feasibility of extraction of energy from the flow by a harmonically oscillating wing is experimentally proved by McKinney and Delaurier [1981]. Jones and Platzer [1997] studied the transition from thrust generation to power generation, and they concluded that if the pitching amplitude is increased to a sufficiently high value, the oscillating wing could extract energy from the flowing fluid. The condition for power generation is that the effective angle of attack must be positive. Plunge amplitude is also one of the significant parameters that should be considered carefully. To achieve sufficient power output, the plunge amplitude is usually have to be comparable to the chord length and the power coefficient linearly increases with the increasing plunge amplitude [Dumas and Kinsey, 2006]. However, the efficiency does not always obey this trend. Kinsey and Dumas [2008] has found that  $90^\circ$  is the optimum phase angle between pitch and plunge for maximum energy extraction. Pivot point location is also very important for a flapping wing power generator. The pivot location has a similar effect as changing the phase angle between pitch and plunge motions [Davids, 1999; Kinsey and Dumas, 2008]. The general summing-up from Davids [1999] and Kinsey and Dumas [2008] is that when the pivot point is just in front of the mid-chord position, the efficiency of power generation takes maximum value. So in this study the pitch pivot point is chosen as  $0.44$  chords ( $c$ ) from the leading edge.

Most investigations on flapping wing power generators are based on sinusoidal motions. However, Platzer et al. [2010] and Ashraf et al. [2011] numerically investigated non-sinusoidal motion of an oscillating-wing power generator with reduced frequency of  $k = 0.8$ , pitching amplitude of  $\theta_0 = 73^\circ$  and plunge amplitude of  $h = 1.05c$ . Their results show that around 17% increase in power generation and

---

<sup>1</sup> Graduate Research Assistant in Astronautical Engineering Department, Email: karakasferhat@itu.edu.tr

<sup>2</sup> Post Doc Researcher/Lecturer in Astronautical Engineering Department, Email: fenercio@itu.edu.tr

around 15% increase in efficiency can be achieved compared to those of sinusoidal motions. Fenercioglu et al. [2015a] experimentally investigated an oscillating-wing power-generator at  $Re=1100$  for the same motion parameters with Platzer [2010] and Ashraf et al. [2011], oscillating with non-sinusoidal pitching and plunging motions about quarter and mid-chords with different stroke reversal times of 0.1 (rapid motion) to 0.5 (sinusoidal motion). There is a good agreement between experimental results and 2D Navier-Stokes simulations. However, in real applications, the end effects due to finite-length wingspan may affect the performance of an oscillating-wing power-generator. Therefore, investigations on the three dimensionality effects needs to be conducted in order to fully understand the physics of the flow around and in the near wake of oscillating wings. Previously, flow structures for a sinusoidally oscillating SD7003 airfoil profile was studied using both two-dimensional and three-dimensional foils with two different aspect ratio values [Caylan et al., 2014]. In order to provide further insight into the 3D effects on an oscillating wing power generator undergoing non-sinusoidal pitch and plunge motions, an experimental investigation is performed in the water channel at the Trisomic laboratory in ITU. The objectives of this study are to understand the effects of three-dimensionality on power extraction from the flowing fluid and the efficiency of oscillating wing power generator undergoing non-sinusoidal pitching and plunging motions about its 0.44 chord length position from the leading edge. The three dimensionality effects of an oscillating-wing power-generator is studied for various stroke reversal times. The objectives of this research are to understand the effect of non-sinusoidal pitching and combined plunging motion parameters on vortex formation for a three dimensional flat plate to provide important information for the design of flapping-wing power generators.

## EXPERIMENTAL SETUP

The Particle Image Velocimetry (PIV) measurements are acquired in the closed-circuit, large scale, free-surface water channel located in the Trisomic Laboratories at the Istanbul Technical University. The test section dimensions are  $1010\text{mm} \times 790\text{mm}$ . The detailed description of the water channel can be found in Fenercioglu and Cetiner [2012; 2014]. Depending on the results from a previous study where different airfoil profiles were tested for sinusoidal flapping motion [Karakas et al., 2014], as well as considering the manufacturing convenience and production costs, the model to be tested is chosen as a non-profiled flat plate. The Plexiglas flat plate with sharp-edged rectangular cross section has chord length of  $c = 10\text{ cm}$  and span of  $s = 30\text{ cm}$  and it is mounted in a vertical cantilevered arrangement about its  $0.44c$  point from leading edge. A connection rod connects the test model to a servo motor to provide a pitching motion via a coupling system which itself is connected to a linear table which provides the plunging motion. In order to reduce the free-surface effects, a rectangular upper end plate with  $30^\circ$  outward bevel is suspended above the vertically mounted flat plate. The lower end plate which was used for 2D study of the flat plate model was removed to investigate the three dimensionality effects of the model, in which case the upper end plate represents the symmetry plane. The experimental setup for three dimensionality effect investigation and the three illumination planes along the span of the flat plate; namely the mid-span ( $1/2$  span), quarter-span ( $1/4$  span) and 2mm above the tip (tip), can be seen in Figure 1a and Figure 1b respectively.

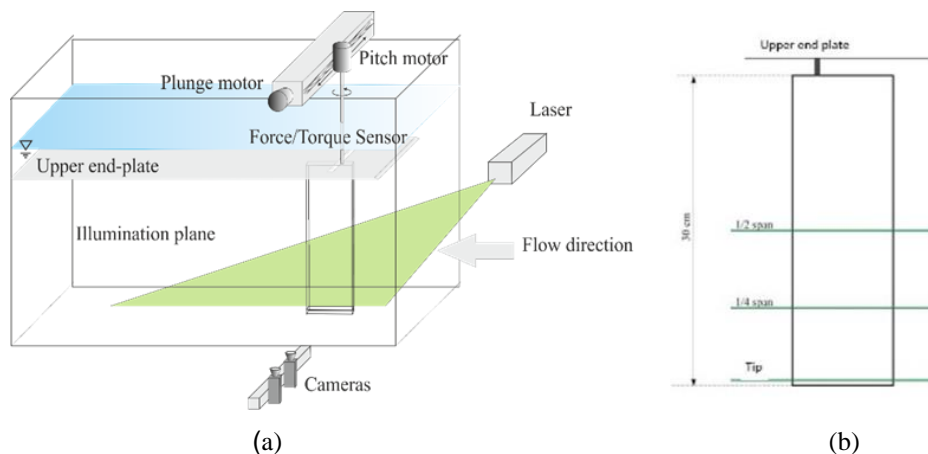


Figure 1. (a) *Experimental Setup*, (b) *Illuminated laser planes*

The PIV system with Dynamic Studio software (Dantec Dynamics A/S) records the detailed vortex formations around and near wake region of the foil. The flow is illuminated by a dual cavity Nd:Yag laser (max. 120 mJ/pulse) and the water is seeded with silver coated glass spheres of  $10\mu\text{m}$  diameter.

Two 10-bit cameras with 1600×1200 pixels resolution were positioned underneath the water channel to capture flow field images and the two double-frame images from the two cameras were stitched before interrogation with an in-house code using two marker points in the illumination plane.

Each experimental data set included 400 instantaneous images which were acquired for 25 cycles of motion. The PIV images were phase-averaged to 16 images to represent one period of the flat plate's motion and interrogated using a double frame, cross-correlation technique with a window size of 64×64 pixels and 50% overlapping in each direction. The resulting measurement plane is represented with approximately 3300 velocity vectors.

A six-component ATI Nano17 IP68 Force/Torque (F/T) sensor (ATI Industrial Automation, Inc.) was used to measure the forces and moments acting on the flapping foil. The sensor was attached to the vertical cantilevered arrangement between the flat plate model and the pitch servo motor, oriented with its cylindrical z-axis normal to the pitch-plunge plane. Dynamic force and moment data was collected for 30 periods with a sampling rate of 10 000 Hz.

## RESULTS

It was shown by Kaya and Tuncer [2007] that nonsinusoidal pitching and plunging motion is optimized for maximum thrust and/or propulsive efficiency. They concluded that, for a maximum thrust generation, the airfoil should stay at about a constant angle of attack during the upstroke and the downstroke motions and reverse direction at the minimum and maximum plunge positions. The non-sinusoidal kinematic motions considered for the flat plate in this study are based on previous studies of Platzer et al. [2010], Ashraf et al. [2011] and Fenercioglu et al. [2015a] where the plunging motion is followed by rapid pitching reversals. The motion of the foil is given in Figure 2, with a period of constant translational velocity combined with a constant pitch angle, followed by a sinusoidal reversal of direction and pitch angle. The motion is accomplished with varying stroke reversal times ( $\Delta T_R$ ) from 0.1 (rapid reversal) to 0.5 (sinusoidal reversal) as a fraction of the total cycle period. The pitch and plunge motions of the airfoil are sustained by Kollmorgen/Danaher Motion AKM33E and AKM54K servo motors respectively.

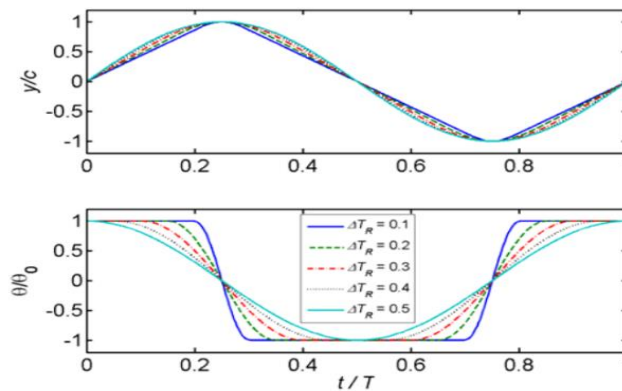


Figure 2. Variation of plunge and pitch motion [Platzer et al. 2009]

The plunge amplitude considered in this study is  $h = 1.05c$  and pitch amplitude is  $\theta_0 = 73^\circ$ . The reduced frequency is kept constant and defined as  $k = 2\pi fc/U_\infty = 0.8$ , where  $U_\infty$  is freestream velocity. In order to obtain the 3D effects and to compare with Fenercioglu et al. [2015b] the chord based Reynolds number for this study is chosen as  $Re = 10\,000$ . The vorticity patterns for a single flat plate pivoting from mid-chord position are given in Figure 3 for half cycle of the flat plate's pitching and plunging motion with phase angle of  $\phi = 90^\circ$  for three pitch stroke reversal times. The first image in each figure shows the flat plate at its mid-plunge position, where it starts its motion ( $t = 0$ ) and the uniform flow is from left to right in the experiments. The flat plate first moves upward and the maximum plunge amplitude position corresponds to the image at  $t = 4T/16$  which is followed by a sinusoidal or rapid pitch reversal depending on  $\Delta T_R$ . The flat plate continues its downward motion after reversal of direction and pitch angle, and the last image for each case at  $t = 7T/16$  shows the test model approaching its mid-plunge position during downstroke. Figure 4 shows the vorticity formations at the mid-span laser plane position for the oscillating 3D flat plate.

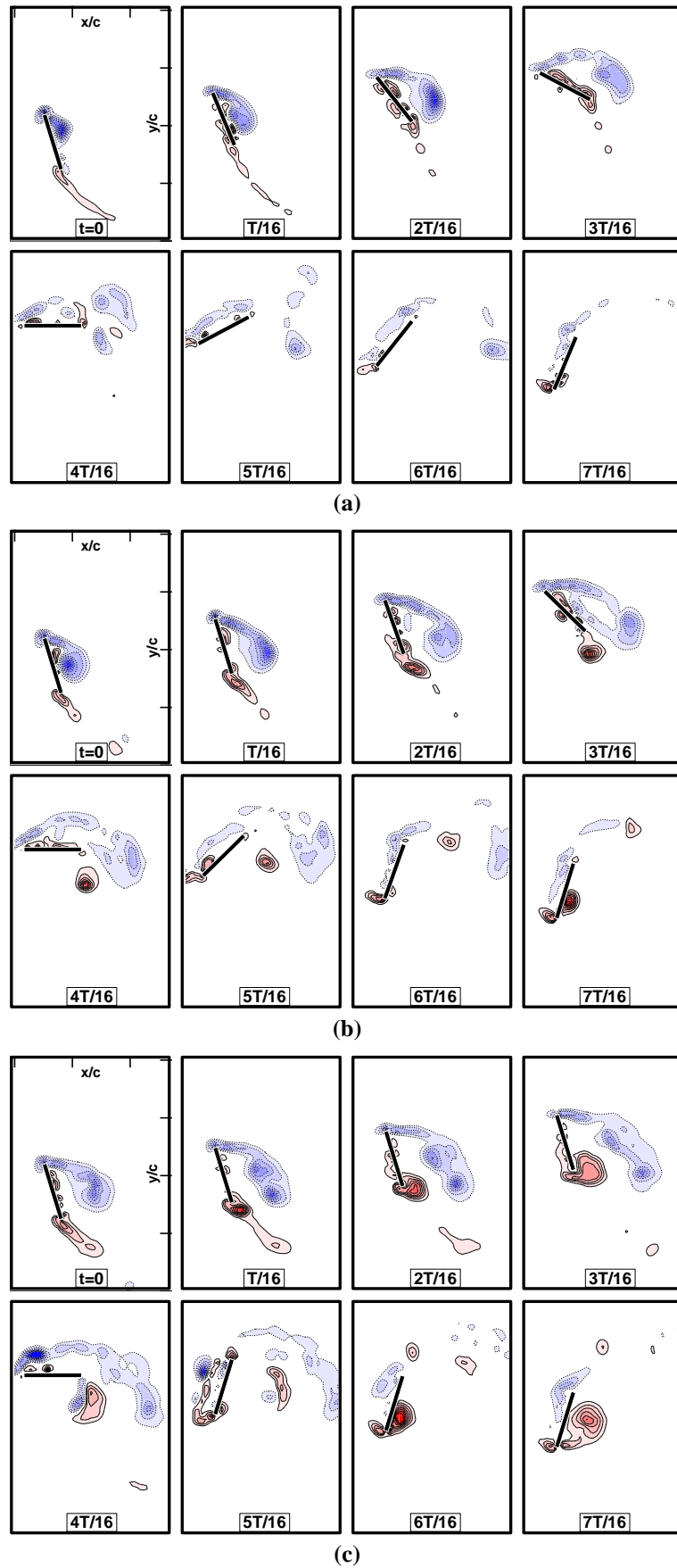


Figure 3. Vorticity patterns for the 2D flat plate,  $Re = 10\ 000$ ,  $k = 0.8$ ,  $h = 1.05$ ,  $\theta_0 = 73^\circ$ ,  $\phi = 90^\circ$ , a)  $\Delta T_R = 0.5$ , b)  $\Delta T_R = 0.3$ , c)  $\Delta T_R = 0.1$  [Fenercioglu et al., 2015b].

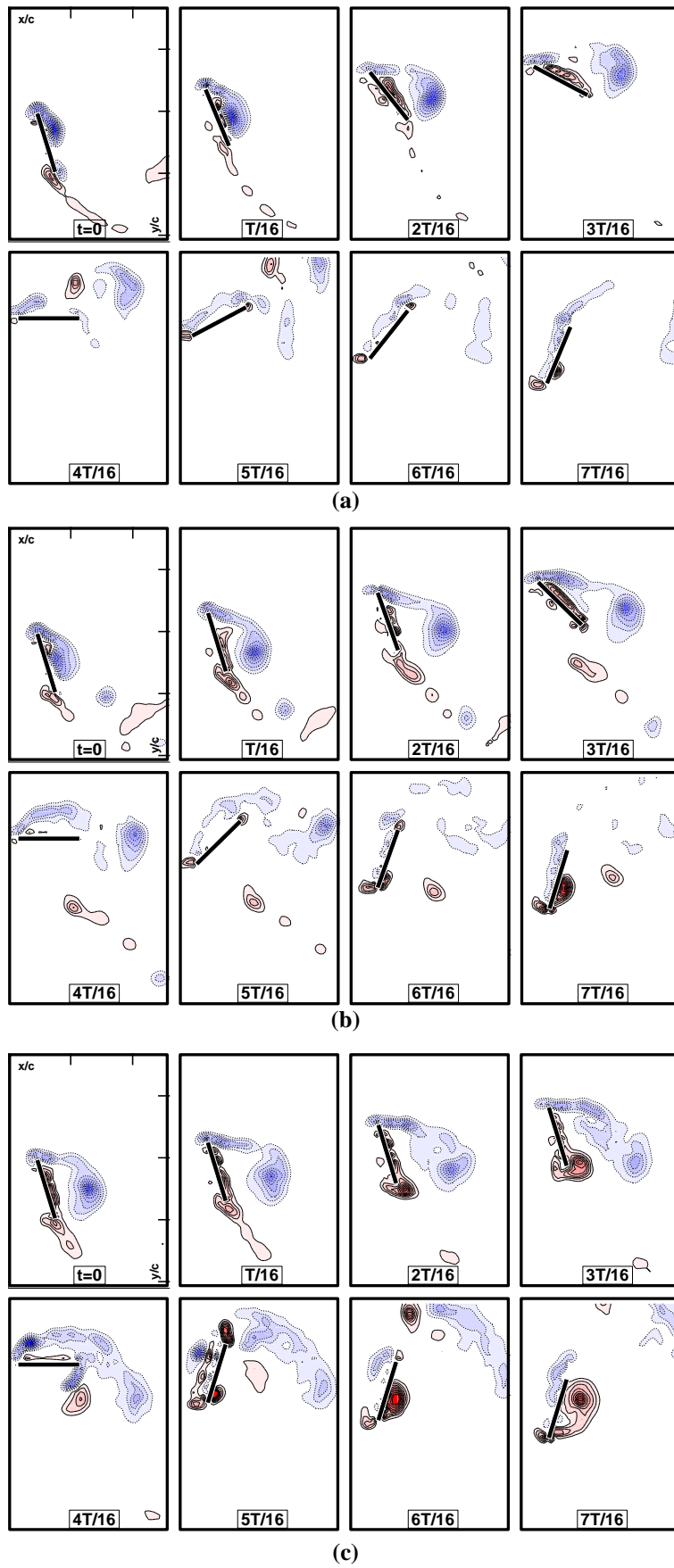


Figure 4. Vorticity patterns at 1/2-span for the 3D flat plate,  $Re = 10\,000$ ,  $\phi = 90^\circ$ , a)  $\Delta T_R = 0.5$ , b)  $\Delta T_R = 0.3$ , c)  $\Delta T_R = 0.1$ .

It can be seen by observing the flow structures around and in the near wake of the flat plate that, the clockwise rotating negative vortex which has started to form on the upper surface of the flat plate from the leading edge at the beginning of the upstroke motion grows as the flat plate continues its upwards motion and sheds into the wake when the foil reaches its maximum plunge amplitude position. Likewise, the counter acting positive vortex forms during the downstroke motion on the flat plate's lower surface. The same formation and shedding of vortices are observed at the mid-span laser plane position for the oscillating 3D flat plate (Figure 4) and both figures reveal that as the rotation speed during stroke reversals is increased so that the stroke reversal time is decreased from  $\Delta T_R = 0.5$  (sinusoidal reversal) to  $\Delta T_R = 0.1$  (rapid reversal), the vortices forming from the leading and trailing edges of the flat plate model also increase the time of their development and are shed earlier into the wake with higher strength. For the sinusoidal pitch rotation case, the negative vortex forming from the leading edge stays closer to the upper surface of the flat plate during its upstroke motion whereas it can be noticed that the negative vortices move away from the flat plate in the cases with non-sinusoidal pitch rotation. It can also be noticed that the counter rotating positive vortex forming on the lower surface of the flat plate is able to curl more and stays closer to the flat plate model for the non-sinusoidal case with highest pitch reversal speed (Figure 4c,  $t = 2T/16$ ) while the same positive vortex dissipates into the wake formed of localized cells of weak vortices for the sinusoidal pitch rotation case (Figure 4a,  $t = 2T/16$ ) as the flat plate approaches its maximum plunge amplitude position during its upstroke motion.

Confirming the results from a previous study where the 2D flat plate's pitch pivot was located at mid-chord (Fenercioglu et al., 2015), the highest mean power coefficient and power extraction efficiency was also observed for pitch stroke reversal time of  $\Delta T_R = 0.3$  and phase angle of  $\phi = 90^\circ$  (Figure 5).

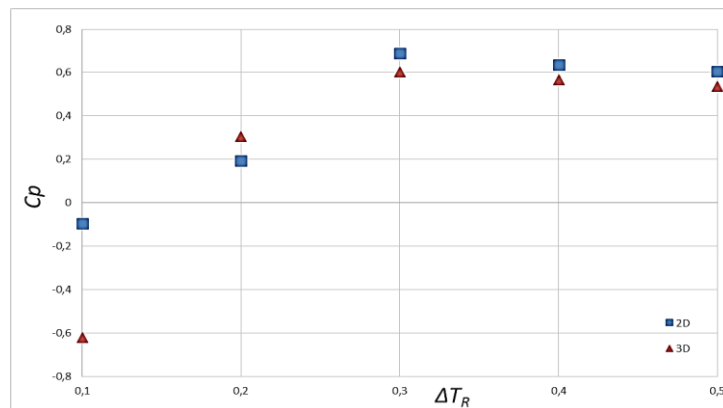


Figure 5. Time averaged power coefficients from direct force measurements for all test cases.

Instantaneous power coefficient graph for the  $\Delta T_R = 0.3$  case in Figure 6 shows that the negative vortex staying closer to the upper surface during the upstroke motion of the flat plate ( $t = 14T/16 - 2T/16$ ) and the counter acting positive vortex formed on the lower side during downstroke ( $t = 6T/16 - 10T/16$ ) enhance to retain power production for an extended amount of time as compared to both the sinusoidal and the rapid pitch reversal cases.

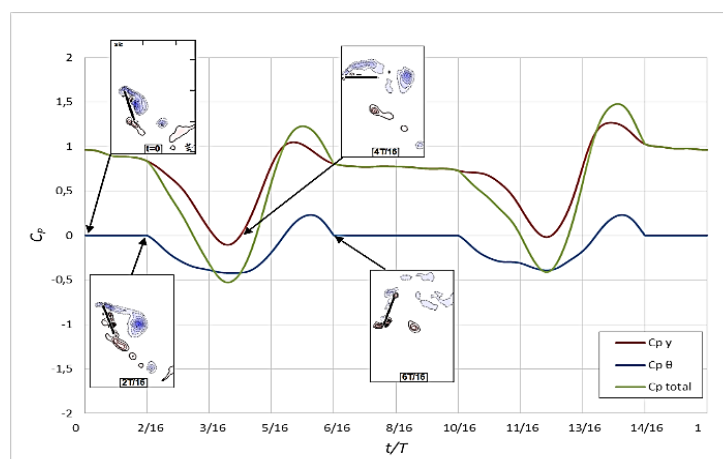


Figure 6. Instantaneous power coefficient for the flat plate with  $\Delta T_R = 0.3$ ,  $\phi = 90^\circ$ .

Although the strength of vorticity formations and the timing of the shedding are quite similar for the 2D oscillating-wing power generator and the 3D finite flat plate when both PIV images are obtained at the mid-span plane, the vorticity patterns acquired at quarter-span and tip of the finite plate visibly reveal the three dimensionality effects. Figure 7 shows the vortical structures acquired at the three illumination planes along the span for the sinusoidally oscillating finite flat plate. It can be observed very clearly that the negative vortex formation on the upper surface of the 3D flat plate experience a pull-down effect along the span at the quarter-span illumination plane where it stays closer to the upper surface and stretches out at the tip of the model. Non-sinusoidal pitch reversal cases also show similar trend; the vortical structures tend to shrink and stick to the upper surface of the flat plate as they move along the span towards the tip, where they stretch out into the wake rather than detach and dissipate (Figures 8 and 9).

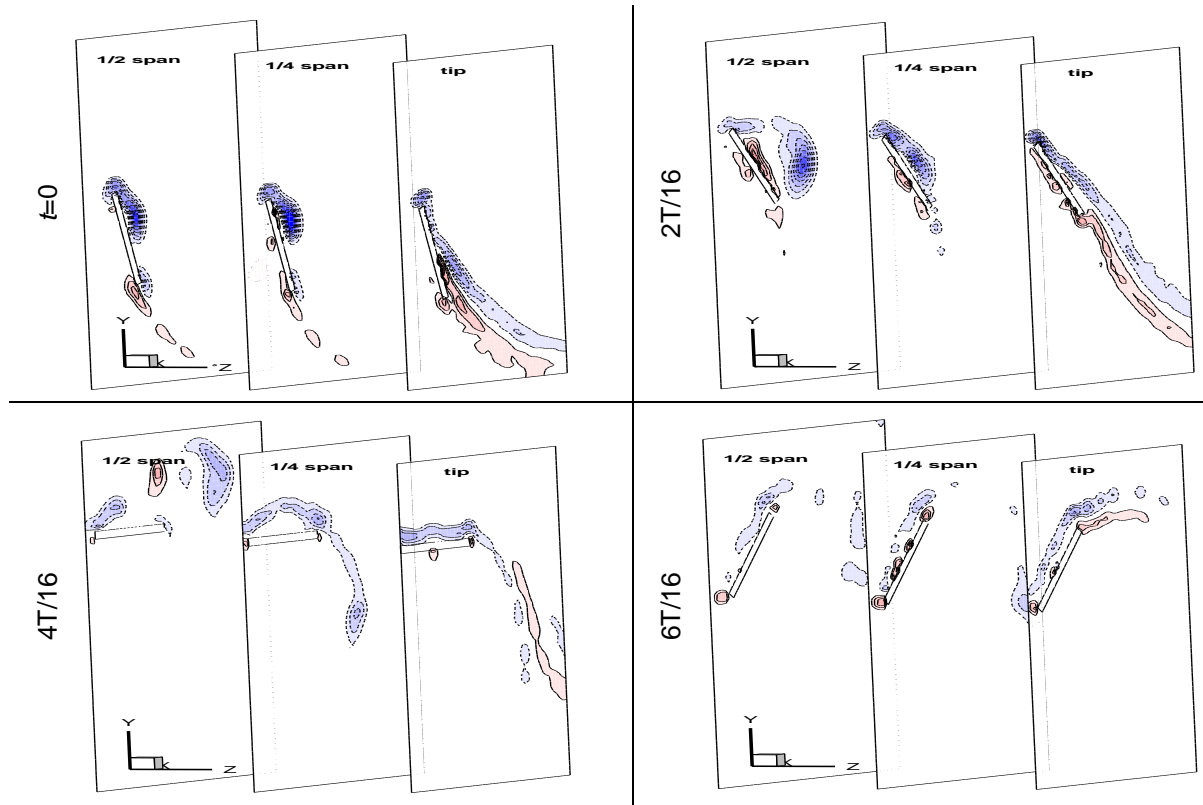


Figure 7. Vorticity patterns at three laser planes along the span of the 3D flat plate,  $\phi = 90^\circ$ ,  $\Delta T_R = 0.5$ .

These findings support Kruyt et al. (2015)'s results where they also identified an attached leading edge vortex (LEV) along the upper surface of their 3D test model which smeared-out and detached outboard. Jones et al. (2011)'s experiments showed minimal interaction between the leading-edge vortices and the tip vortex for sliding wings however they observed notable spanwise flow on low aspect ratio waving wings. They reported that the shed vortices tend to lift off the wing surface near the wing tip, but remain close to the surface further inboard; as also observed in our cases (e.g. Figure 8,  $t = 2T/16$ ), where the negative LEV stays closer to the upper surface at the 1/4-span plane, and lifts off the surface at the tip plane. In a previous study by Caylan et al. (2014), the flow was found to be mainly two dimensional over most of the wing span for higher aspect ratio finite wing and three-dimensionality effects were mostly observed for the shorter model, where the kinematic motion was combined sinusoidal pitching and plunging with a lower pitch amplitude than the present study. Kruyk et al. (2015)'s latest research show the outboard flow separation on high aspect ratio wings at high angle of attack values.

The efficiency results in Figure 10 also imply the effects of three-dimensionality, where the flow separates and forms a tip vortex which interferes with the wake of the flat plate, thus reducing the overall efficiency for all cases, except for the  $\Delta T_R = 0.2$  case.

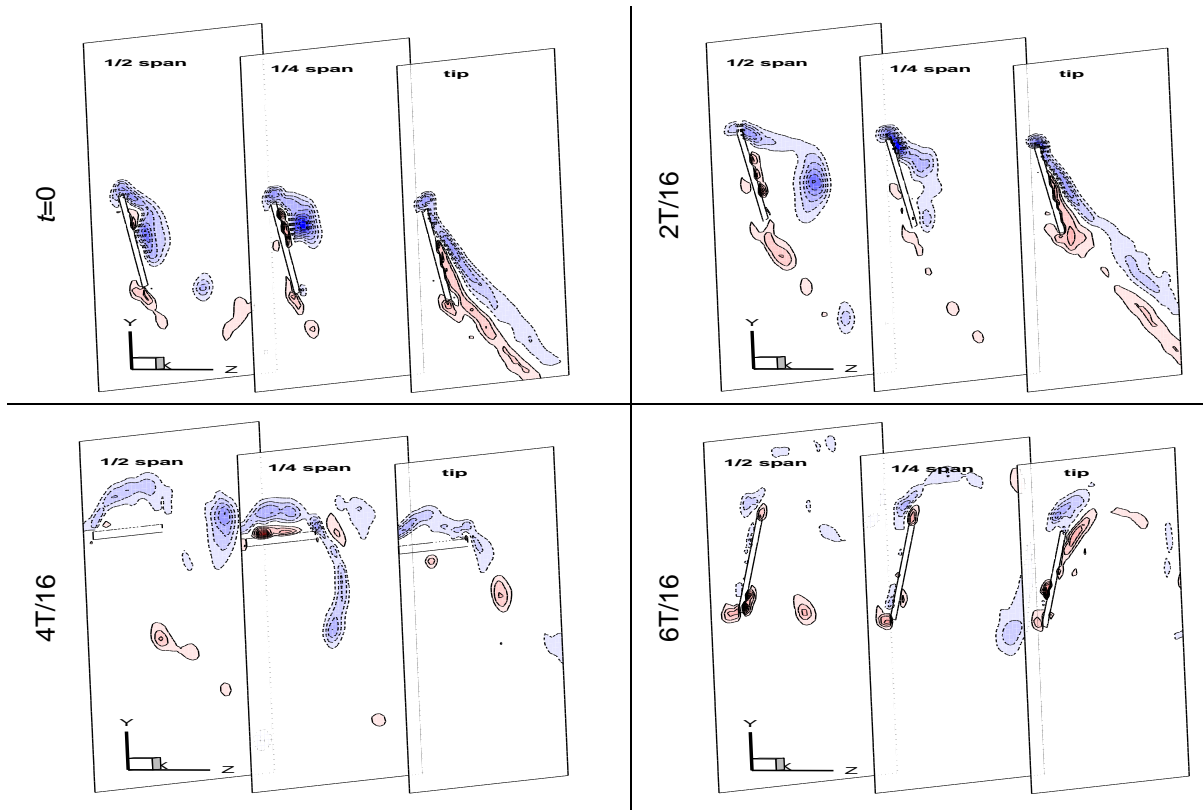


Figure 8. Vorticity patterns at three laser planes along the span of the 3D flat plate,  $\phi = 90^\circ$ ,  $\Delta T_R = 0.3$ .

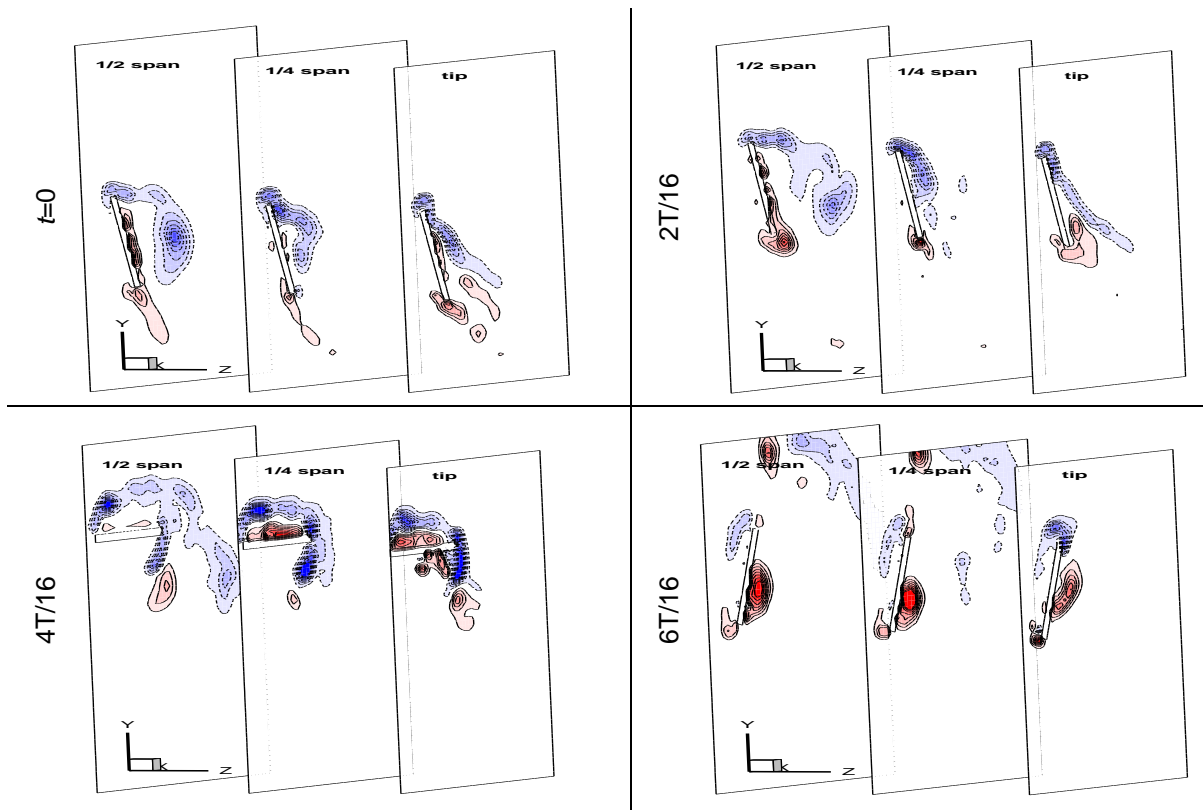


Figure 9. Vorticity patterns at three laser planes along the span of the 3D flat plate,  $\phi = 90^\circ$ ,  $\Delta T_R = 0.1$ .



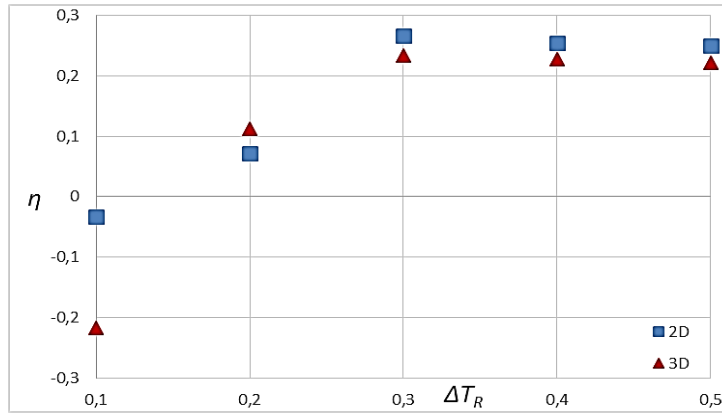


Figure 10. Efficiency for 2D and 3D flat plate for all pitch stroke reversal times,  $\phi = 90^\circ$ .

## CONCLUSIONS

An experimental investigation via quantitative flow visualizations and simultaneous direct force measurements were performed using a flat plate to model an oscillating-wing power-generator undergoing non-sinusoidal pitch leading plunge motions with phase angle of  $\phi = 90^\circ$  about its 0.44c pitch pivot point from the leading edge with stroke reversal times of 0.1 (rapid reversal) to 0.5 (sinusoidal reversal). The experiments took place in a water channel using a test model with rectangular cross section in two-dimensional and a three-dimensional setup. The flat plate has fixed chord length based Reynolds number of  $Re = 10\,000$ , reduced frequency of  $k = 0.8$ , plunge amplitude of 1.05 chords and pitch amplitude of  $73^\circ$  throughout the experiments. The evolutions of vortical structures were recorded at three illumination planes in the spanwise direction to comment on the three dimensionality effects.

The flow structures around and in the near wake of the flat plate show that, as the rotation speed during stroke reversals is increased, the vortices are shed earlier into the wake with higher strength. For rapid reversals ( $\Delta T_R = 0.1$ ), none of the test cases were capable to produce a positive mean power coefficient. The highest mean power coefficient and power extraction efficiency was observed for three dimensional case with pitch stroke reversal time of  $\Delta T_R = 0.3$  and phase angle of  $\phi = 90^\circ$ , which confirms the results from a previous study for two dimensional test model with mid-chord rotation (Fenercioglu et al., 2015).

Although the formation and shedding of vortical structures in the mid-span plane are quite similar with 2D cases, the three dimensionality effects are visible at quarter-span and the tip of the flat plate. In three dimensional cases, LEV and tip vortex interactions create shrinkage in size in the vortical structures at the upper surface where they tend to stay closer to the flat plate. The separated tip vortex interferes with the wake of the flat plate, thus reduces the overall efficiency.

## Acknowledgements

This study is supported by ITU-BAP Grant No. 37631 and TUBITAK Grant No. 214M385.

## References

- Ashraf, M., Young, J., Lai, J., and Platzer, M. (2011). *Numerical analysis of an oscillating-wing wind and hydropower generator*. AIAA Journal, Vol. 49(7), p:1374-1386.
- Çaylan, U., Seçkin, S., Köse, C., Son, O., Zaloğlu, B., Fenercioglu, İ., and Çetiner, O. (2014). *Çırpınan kanatta üç boyutluluk etkisi*. İstanbul: Ulusal Havacılıkta İleri Teknolojiler Konferansı, HİTEK-2014-094.

- Dauids, S. T. (1999). *A Computational and Experimental Invetigation of a Flutter Generator* . Naval Postgraduate School, Master's thesis.
- Dumas, G., and Kinsey , T. (2006). *Eulerian simulations of oscillating airfoils in power extraction regime*. Advances in fluid mechanics ; 6<sup>th</sup> International conference Advances in fluid mechanics, 52, p:245-254.
- Fenercioglu, I., and Cetiner , O. (2012). *Categorization of flow structures around a pitching and plunging airfoil*. Journal of Fluids and Structures, Vol. 31, p:92-102.
- Fenercioglu, I., and Cetiner, O. (2014). *Effect of unequal flapping frequencies on flow structures*. Aerospace Science and Technology , Vol. 35, p:39-53.
- Fenercioglu, I., Zaloglu, B., Young, J., Ashraf, M. A., Lai, J., and Platzer, M. (2015a). *Flow Structures Around an Oscillating-Wing Power Generator*. AIAA Journal, Early Edition, published online 26 March 2015, p:1-11.
- Fenercioglu, I., Zaloglu, B., Ashraf, M. A., Young, J., and Platzer, M. F. (2015b). *Flow around an Oscillating Tandem-Wing Power Generator*. 53<sup>rd</sup> AIAA Aerospace Sciences Meeting (SciTech2015) Science and Technology Forum and Exposition, AIAA-2015-1751.
- Jones, AR., Pitt Ford, CW., Babinsky, H. (2011). *Three-Dimensional Effects on Sliding and Waving Wings*. Journal of Aircraft, Vol. 28(2), p:633-644.
- Jones , K., and Platzer, M. (1997). *Numerical Computation of Flapping-wing Propulsion and Power Extraction* . 35<sup>th</sup> Aerospace Sciences Meeting and Exhibit, AIAA-97-0826.
- Karakaş, F., Paça , O., Köse, C., Son, O., Zaloğlu, B., Fenercioglu, İ., and Çetiner, O. (2014). *Çırpan kanatta kanat profilinin etkisi* . Havacılık ve Uzay Teknolojileri Dergisi , Vol. 7(2), p:55-70.
- Kaya, M., and Tuncer, I. (2007). *Nonsinusoidal Path Optimization of a Flapping Airfoil*. AIAA Journal, Vol. 45(8), p:2075-2082.
- Kinsey , T., and Dumas, G. (2008). *Parametric study of an oscillating airfoil in a power-extraction regime*. AIAA Journal , Vol. 46(6), p:1318-1330.
- Kruyt JW, van Heijst GF, Altshuler DL, Lentink D. (2015). *Power reduction and the radial limit of stall delay in revolving wings of different aspect ratio*. Journal of Royal Society Interface, Vol. 12, p:20150051.
- McKinney , W., and DeLaurier, J. (1981). *The wingmill: an oscillating-wing wind-mill*. Journal of Energy, Vol. 5, p:109-115.
- Platzer, M., Ashraf, M., Young , J., and Lai, J. (2010). *Extracting power in Jet streams: pushing the performance of flapping wing technology*. 27<sup>th</sup> International Congress of the Aeronautical Sciences, ICAS 2010-2.9.1.